ЖЭТФ, 2005, том 127, вып. 2, стр. 471–477

PYROELECTRIC AND ELECTROMECHANICAL PROPERTIES OF ANTIFERROELECTRIC LIQUID CRYSTAL MHPOBC

S. V. Yablonskii [*a,b], ***K. Nakano*** [a], ***M. Ozaki*** [a], ***K. Yoshino*** [a]

[a] *Department of Electronic Engineering, Graduate School of Engineering, Osaka University*
2-1 Yamada-Oka, Suita, Osaka 565-0871, Japan

[b] *Institute of Crystallography, Russian Academy of Science*
117333, Moscow, Russia

Submitted 30 June 2004

We study pyroelectric and electromechanical effects in the prototype antiferroelectric liquid crystal 4-(1-methylheptyloxycarbonyl-phenyl)4′-octylbiphenil-4-carboxylate (MHPOBC). The linear electromechanical effect in the freely suspended liquid crystal films of MHPOBC has been detected in the broad temperature range inclusive of the antiferroelectric SmC_A^* as well as paralelectric SmA. The anomalous behavior of the hysteresis loop of SmC_β^* in the (pyroelectric coefficient, dc bias electric voltage) coordinates has been found.

PACS: 64.70.Md, 68.15.+e, 62.30.+d

1. INTRODUCTION

Antiferroelectricity of a liquid crystal was first discovered in 4-(1-methylheptyloxycarbonyl-phenyl)4′-octylbiphenil-4-carboxylate (MHPOBC) [1, 2]. This material has three chiral smectic subphases (SmC_α^*, SmC_β^*, and SmC_γ^*) between paraelectric SmA and antiferroelectric SmC_A^*. The arrangements of the molecules in these phases are shown in Fig. 1. Different experimental techniques, such as resonant x-ray scattering [4], dielectric spectroscopy [5, 6], optical rotation [7], conoscopic observation [8], ellipsometry on freely suspended films [9], differential scanning calorimetry [10], and electric current and optical transmittance responses [1, 11] have been used to identify and characterize the structure of these phases.

In chiral mesophases, a spontaneous polarization arises as a secondary order parameter due to a molecular tilt with respect to the smectic layer normal; the $\mathbf{P}_s$ vector lies in the tilt plane, reflecting the polar properties of a liquid crystal [12]. Chirality plays a crucial role for the emergence of polarization in the direction of the tilt plane normal. In smectic phases, where rodlike molecules are organized into fluid stacks of planar layers, weak chiral twisting forces induce a helical order with the helical axis parallel to the layer normal. The resulting helical pitch is in the optical wavelength range. If the pitch is large, it is easy to unwind the helix by application of a weak strain, for example, imposed by a mechanical shear or by a weak applied electric field. Then the sample has a ferroelectric response under moderate applied electric and mechanical fields.

In this paper, the polar properties of chiral smectic subphases of the classic antiferroelectric liquid crystal MHPOBC are investigated by recording its pyroelectric coefficient and studying the vibration of freely suspended films induced by alternating electric voltage (the so-called linear electromechanical effect) [13]. The pyroelectric activity of the «unwound» chiral liquid crystal confirms the polar structure of mesophases, whereas the thermal behavior of the linear electromechanical response reveals specific features related to phase transitions of smectic subphases and their structure.

2. EXPERIMENTAL

2.1. Pyroelectric set-up and cell

To study the antiferroelectric and ferrielectric behavior of our material, we used a pulse pyroelectric setup shown in Fig. 2 [14]. A 100μs pulse of a Nd^{3+} YAG laser was used to provide a small local temperature

*E-mail: lbf@ns.crys.ras.ru

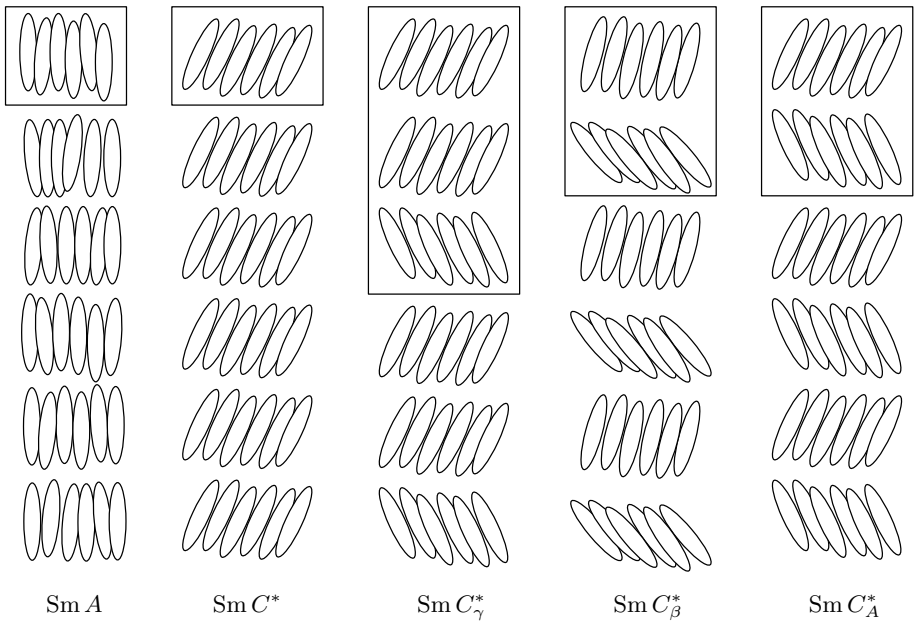

Fig. 1. Model structures of the paraelectric SmA, ferroelectric SmC^*, ferrielectric SmC^*_γ, SmC^*_β, and antiferroelectric SmC^*_A phases. The unit cells are marked by frames. In SmC^*_α (not shown in the picture), the superlattice incommensurate period (corresponding to the helical pitch) ranges between 5 and 8 smectic layers [3]

change in the sample. Laser radiation ($\lambda = 1.06\mu$m) was partly absorbed in indium-tin-oxide (ITO) layers. The pyroelectric response was measured as a pulse voltage across the load resistor $R_L = 100\ k\Omega$ with a wide-band amplifier and a storage oscilloscope. A dc field of various strengths was applied to the sample in order to measure hysteresis loops in the coordinates (pyroelectric response, dc bias voltage).

The temperature dependence of the spontaneous polarization (on an arbitrary scale) was calculated by integrating the pyroelectric coefficient γ in accordance with the expression [14]

$$P_s(T) = \int_{T_i}^{T} \gamma(T)\, dT, \qquad (1)$$

where T_i is the temperature of the transition to the paraelectric phase. Then the correct scale for γ and P_s was introduced by comparison of the pyroelectric response at a certain temperature with the value measured for a well-known ferroelectric liquid crystal. Strictly speaking, Eq. (1) is valid only for the field-off regime. When an external dc field is applied to prepare a ferroelectric monodomain or an «unwound» antiferroelectric (or ferrielectric), the actually measured quantity is the total polarization $\mathbf{P} = \mathbf{P}_s + \mathbf{P}_i$, where $\mathbf{P}_i$ is the field-induced contribution, for example, observed in the isotropic phase. Because $\mathbf{P}_i$ is much smaller than $\mathbf{P}_s$, we can use Eq. (1) for the measurements of $\mathbf{P}_s$ in the «unwound» antiferroelectric phase.

The shape of the hysteresis loop is one of the major criteria to refer the nonlinear dielectrics to ferro-, ferri- or antiferroelectric types. Hysteresis loops are usually represented in coordinates of the electric displacement against the external electric field. But it is possible to demonstrate that the representation of hysteresis loops in the coordinates given by the pyroelectric coefficient vs the external electric field differs only quantitatively. Indeed, using the definition of the volume polarization $P_s = (N\mu/V)\langle\cos\varphi\rangle$ and the pyroelectric coefficient

$$\gamma = \frac{d\mu}{dT}\,\frac{N}{V}\,\langle\cos\varphi\rangle,$$

where N is the number of dipoles of moment μ within the volume V and $\langle\cos\varphi\rangle$ is the average value of the cosine of the angle between the dipole direction and the net polarization direction, we can deduce that the ratio P_s/γ is constant at a given temperature.

2.2. Linear electromechanical effect in ferroelectric freely suspended film

Unlike in the standard case of a liquid crystal sample in a confined geometry, the surface of a freely suspended liquid crystal film can easily be deformed under

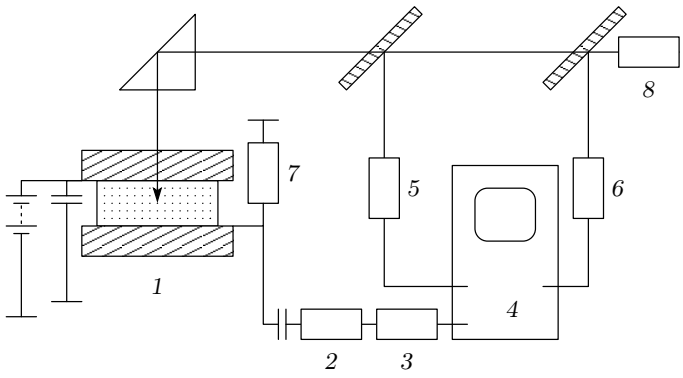

Fig. 2. Pulse pyroelectric set-up: *1* — liquid crystal cell, *2* — amplifier, *3* — time-delay line, *4* — oscilloscope, *5* — photomultiplier to control the form of the laser pulse, *6* — photomultiplier to start-up the line scanning, *7* — load resistor (100 $k\Omega$), *8* — YAG laser

the action of weak acoustic or electric fields [15, 16]. Such a film is considered a perfect membrane, whose vibrational motion depends only on the film geometry, the isotropic surface tension σ, and the homogeneous two-dimensional density ρ_s (including the inertia of the air moving with the film) [17]. For excitation of the transverse film vibrations, a linear coupling of the lateral electric field to the spontaneous polarization of a ferroelectric liquid crystal has been exploited [13]. In the experiment, the azimuthal motion of the liquid crystal director is accompanied by the so-called backflow, which induces viscous stress acting on the film surface as shown in Fig. 3. This mechanism assumes a velocity gradient along the normal to the film surface, which implies the presence of an internal structure in freely suspended films. The resulting film deformation strongly depends on the surface viscosity of the liquid crystal and also on the value and sign of spontaneous polarization. This combination of properties makes the measurements of freely suspended film oscillations a useful tool for studying the spontaneous polarization phenomenon in liquid crystals [13].

The periodical displacement of the film surface results in deflection of the probing beam of a low-power He-Ne laser (Fig. 4). By passing the beam through an iris diaphragm, the deflection of the beam is converted into an amplitude modulation of the laser intensity, detected by a photodiode. The photodiode response current is analyzed by a lock-in amplifier tuned to the first harmonic of the control voltage. Microscope observations were carried out by inserting the sample holder on the turntable of the polarization microscope.

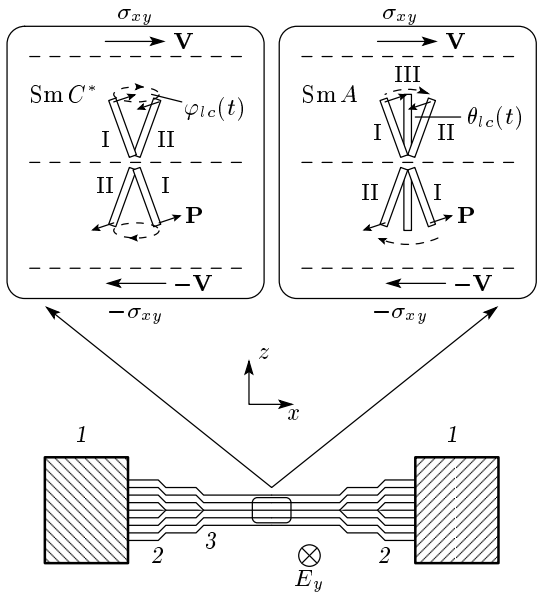

Fig. 3. Schematic representation of a smectic liquid crystal freely suspended film: *1* — frame, *2* — meniscus, *3* — uniform part of the freely suspended film. The insets illustrate a mechanism responsible for the development of a viscous stress σ_{xy} in both ferroelectric and paraelectric phases. $\varphi_{lc}(t)$ and $\theta_{lc}(t)$ are the recpective variable azimuthal and zenithal angles. $\mathbf{V}$ is the liquid crystal velocity field, inhomogeneous along the z axis, $\mathbf{P}$ is the spontaneous polarization. Roman numerals I and II correspond to the respective positions of liquid crystal molecules for the positive and negative electric field

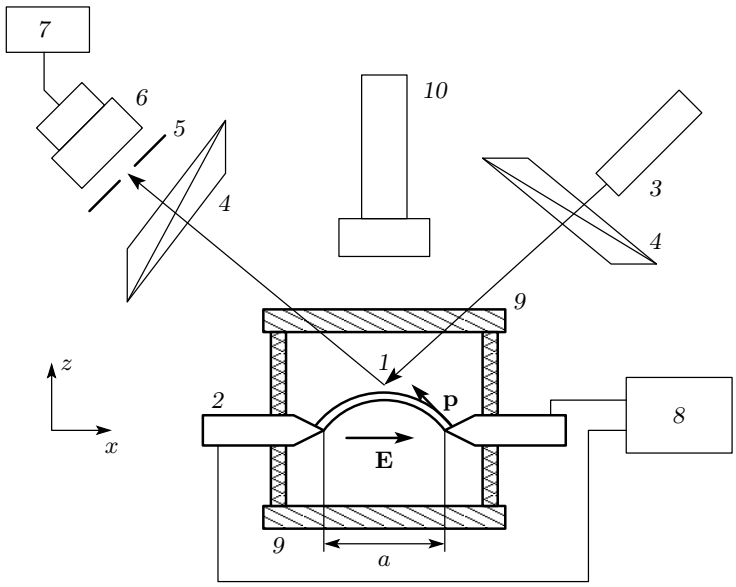

Fig. 4. Experimental set-up for the study of the linear electromechanical effect in freely suspended films. *1* — ferroelectric freely suspended liquid crystal film (MHPOBC), *2* — two Au electrodes, *3* — He-Ne laser (s-polarization), *4* — two polarizers, *5* — slit diaphragm, *6* — photodiode, *7* — lock-in amplifier, *8* — audio frequency generator, *9* — two glasses placed near the film surfaces to prevent the influence draughts, *10* — polarization microscope

2.3. Materials and samples

The antiferroelectric liquid crystal used in our experiment is S-MHPOBC with a moderate spontaneous polarization (about 70 nC/cm^2 at 112 °C) and the following sequence of phase transitions:

$$\text{Iso-(149.8 °C)-Sm}A\text{-(122 °C)-Sm}C^*_\alpha\text{-(120.9 °C)-}$$
$$\text{-Sm}C^*_\beta\text{-(119.2 °C)-Sm}C^*_\gamma\text{-(118.4 °C)-Sm}C^*_A.$$

For pyroelectric measurements, the liquid crystal was introduced in a flat capillary cell made up of ITO-covered, nontreated glass plates with 10 μm thick Teflon spacers. ITO surfaces were cleaned with acetone and used without any orienting layers. The cell (with the area between electrodes $A = 5 \times 5$ mm^2) was filled with the liquid crystal in the isotropic phase. Cells were placed in a thermal jacket with optical windows.

The electromechanical effect was studied in freely suspended films fabricated by the standard procedure described in [18]. The experiment was performed with a glass frame of fixed geometry (rectangular slit with the area 2×10 mm^2 and the thickness 1 mm). The frame with a spanned film of MHPOBC was mounted in a heating stage and the film could be stabilized at a given temperature to ±0.3 °C.

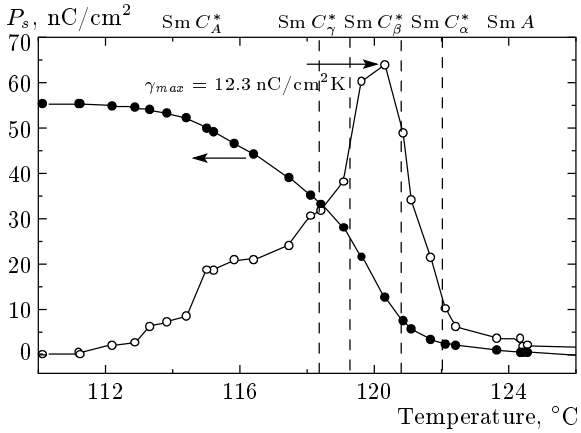

Fig. 5. The pyroelectric coefficient γ (open circles) and the spontaneous polarization P_s (filled circles) of 10 μm-thick cell measured as functions of temperature for the bias dc voltage 10 V

3. RESULTS AND DISCUSSIONS

Figure 5 presents the results of the measurements of the pyroelectric coefficient γ and spontaneous polarization P_s as functions of the temperature obtained in cooling process. In Fig. 5, from the analysis of the pyroelectric curve, we can clearly distinguish three ferrielectric phases (SmC^*_α, SmC^*_β, and SmC^*_γ) from SmA

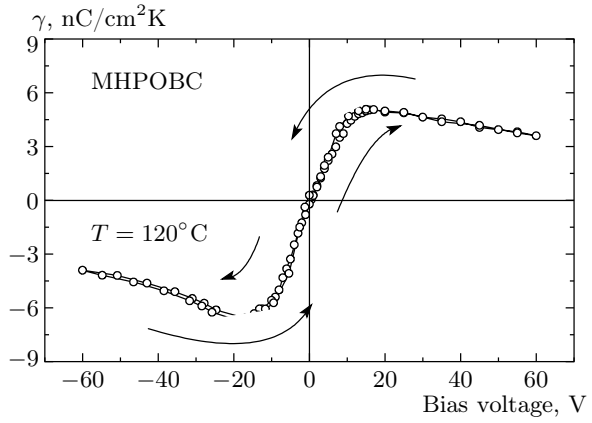

Fig. 6. Hysreresis loop in the coordinates (pyroelectric coefficient, bias dc voltage) for MHPOBC measured at the fixed temperature $T = 120\,^{\circ}$C corresponding to the SmC^*_β phase. Arrows show the direction of the round

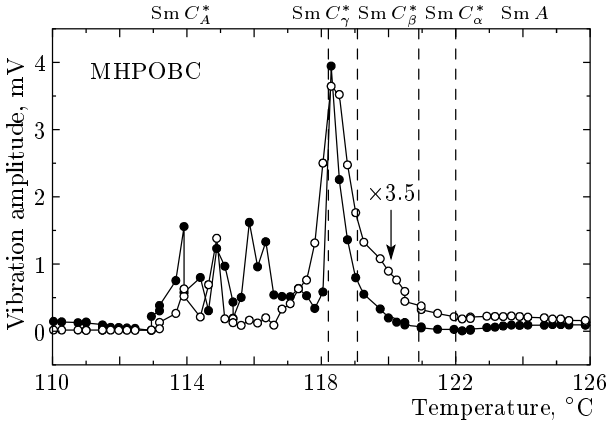

Fig. 7. Temperature dependence of the vibration amplitude in a freely suspended film in MHPOBC of the linear (filled circles) and quadratic (open circles) electromechanical effects. Quadratic amplitudes were multiplied by the factor 3.5. The cooling rate is $5\,^{\circ}$C/min with the temperature resolution $0.3\,^{\circ}$C. The rectangular film size is 2×10 mm^2 ($a = 2$ mm, $b = 10$ mm). The number of layers is $N = 205$. Sinusoidal voltage with the amplitude $U = 115$ V and frequency $\nu = 2200$ Hz was applied to electrodes. A photovoltage of 10 mV corresponds to displacement of the film surface by 800 nm

and SmC^*_A. According to this plot, the pyroelectric signal is detectable not only in polar ferriellectric phases but also in antiferroelectric SmC^*_A. The pyroelectric signal in these phases appears to be due to a distortion of the helical structure induced by the external electric field. The maximum of the pyroelectric effect occurs in ferrielectric SmC^*_β (which some authors identified as SmC^* [19]) at $T = 120.3\,^{\circ}$C. It is interesting to note that the temperature dependence of the real part of the dielectric constant of MHPOBC peaked at the same temperature [20]. A similar behavior has also been detected in other antiferroelectric systems [21].

The polarization shown in Fig. 5 is obtained by integrating the pyroelectric coefficient over temperature, starting from the temperature $T_0 = 126\,^{\circ}$C, about $4\,^{\circ}$C above the transition from paraelectric SmA to ferrielectric SmC^*_α: a small pyroelectric signal induced by the field in SmA (about 0.04 nC/cm$^2 \cdot$ K) was subtracted as a background value. The maximum value of polarization in SmC^*_A of 60 nC/cm^2 is comparable with that obtained by the repolarization current technique [22].

The bias dependence of the sum of the induced and spontaneous pyroelectric coefficients mearured at $T = 120\,^{\circ}$C in SmC^*_β is shown in Fig. 6. This plot drastically differs from the standard hysteresis loop of solid ferroelectrics [23]. First of all, the hysteresis loop shrinks to a thin line, which is typical of ferroelectric liquid crystal materials, where dipoles are ordered in a helical fashion [24]. Second, the nonmonotonic behavior of the pyroelectric signal, shown in this plot, is not common for solid and liquid ferroelectrics. The initial linear growth corresponding to the helix distortion is followed by the decrease of the pyroelectric response at elevated bias field. A decrease in the pyroelectric response with a further increase in the field can be a consequence of two reasons. One of them is explained in [21] as the effect of the competition between the induced and spontaneous polarizations having the opposite signs of the pyroelectric coefficients. The other cause can be connected with the electroclinic effect, promoting the decrease of pyroelectric response with the increasing dc bias voltage [25].

Figure 7 demonstrates the temperature dependence of the linear and quadratic electromechanical effects in a relatively thick, about 800 nm, freely suspended film made from MHPOBC. Such a thickness corresponds approximately to two complete turns of the natural smectic helix in long-pitch phases. According to these plots, the linear and quadratic electromechanical effects are present in all phases (with the exception of SmC^*_α in the case of the linear electromechanical effect). The linear effect is rather strong in SmC^*_β, SmC^*_γ, and (unexpectedly) SmC^*_A. The temperature dependence of the quadratic electromechanical effect correlates closely with the temperature dependence of the real part of the dielectric permittivity [20]. This condition is not occasional but simply reflects the influence of the dielectric

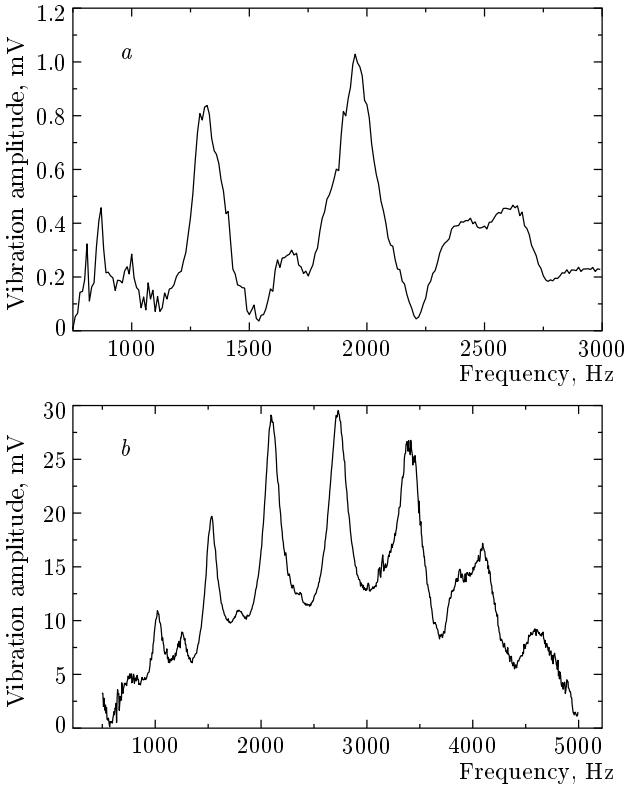

Fig. 8. Spectra of the linear electromechanical effect in a freely suspended film due to: the electroclinic effect (a), $T = 135\,^{\circ}$C (SmA) and the ferroelectric switching (b), $T = 114.5\,^{\circ}$C (SmC^*_A). MHPOBC, $N = 205$, $U = 115$ V

torque, quadratic in the electric field, on the shape of the film surface. Thus, the cause of the quadratic effect in a freely suspended film is electrostriction, whereas the dominating ferroelectric torque is responsible for the linear effect in unwound ferroelectrics. In the general case of chiral smectics, one should also take flexoelectric and «electroclinic» torques into account. (We use «electroclinic» in quotation marks because the electric field exerts no torque on the director in the electroclinic action but influences only the whole medium, shifting the direction of the equilibrium in space [24]). Obviously, the linear electromechanical effects, shown in Fig. 8, in antiferroelectric SmC^*_A and paraelectric SmA are due to the influence of the sum of the flexoelectric and «electroclinic» torques. The external torques induce a «back-flow», which is linearly coupled with a mechanical stress tensor [26]. Accordingly, the films vibrate with the fundamental and double frequencies of the applied ac electric field.

As one can see in Fig. 7, the linear electromechanical effect is absent in incommensurate tilted SmC^*_α. This phase has an extremely short helical period that typically extends over ten smectic layers and, consequently, requires large power expenses for its disturbance, which evidently could not be realized by relatively weak lateral electric fields used in the experiment (of the order 0.05 V/μm). The difficulty of the generation of the linear effect is also favored by smallness of the spontaneous polarization in SmC^*_α, as one can see in Fig. 5, and space averaging of the flexoelectric and spontaneous polarization over the chiral structure.

4. SUMMARY

In conclusions, by pyroelectric and electromechanical methods sensitive to both the polar and non-central-symmetric ordering of molecules in liquid crystalline media, we investigated the prototype antiferroelectric liquid crystal MHPOBC. Our observations confirm the polar properties of MHPOBC in ferrielectric phases and in the «unwound» antiferroelectric state. We also found that MHPOBC manifests a linear electromechanical effect in unpolar non-central-symmetric SmA and SmC^*_A. This phenomenon can be interpreted as the effect of electroclinic and flexoelectric tourqes. In addition, we did not succed in observation of the linear electromechanical effect in noncommensurate SmC^*_α, which is seemengly connected with its nano-scale orientational order.

We acknowledge financial support from a Grant-in-Aid for Scientific Research from Ministry of Education, Science, Sports, and Culture. One of the authors (S. V. Ya.) thanks the Japanese Society for Promotion of Science for a Fellowship at Osaka University and the RFBI (grants Nos. 03-02-17288 and 04-02-16466).

REFERENCES

1. A. D. L. Chandani, T. Hagiwara, Y. Suzuzki, Y. Ouchi, H. Takezoe, and A. Fukuda, Jpn. J. Appl. Phys. **27**, L729 (1988).

2. A. D. L. Chandani, E. Gorecka, Y. Ouchi, H. Takezoe, and A. Fukuda, Jpn. J. Appl. Phys. **35**, 5054 (1996).

3. V. Laux, N. Isaert, V. Faye, and H. T. Nguen, Liq. Cryst. **27**, 81 (2000).

4. P. Mach, R. Pindak, A. M. Levelut, P. Barois, H. T. Nguen, C. C. Huang, and L. Furenlid, Phys. Rev. Lett. **81**, 1015 (1998).

5. K. Hiraoka, A. Taguchi, Y. Ouchi, H. Takezoe, and A. Fukuda, Jpn. J. Appl. Phys. Pt. 2, **29**, L103 (1990).

6. K. Hiraoka, Y. Takanishi, H. Takezoe, A. Fukuda, T. Isozaki, Y. Suzuki, and I. Kawamura, Jpn. J. Appl. Phys. **31**, 3394 (1992).

7. I. Musevic and M. Skarabot, Phys. Rev. E **64**, 051706 (2001).

8. H. Takezoe, J. Lee, A. D. L. Chandani, E. Gorecka, Y. Ouchi, A. Fukuda, K. Terashima, and K. Furukawa, Ferroelectrics **114**, 187 (1991).

9. D. Schlauf, Ch. Bahr, and H. T. Nguen, Phys. Rev. E **60**, 6816 (1999).

10. M. Fukui, H. Orihara, Y. Yamada, N. Yamammoto, and Y. Ishibashi, Jpn. J. Appl. Phys. **28**, L849 (1989).

11. M. Kimura, D. Kang, and C. Rosenblatt, Phys. Rev. E **60**, 1867 (1999).

12. R. B. Meyer, L. Liebert, L. Strzelecki, and P. Keller, J. de Phys. Lett. **36**, 69 (1975).

13. S. V. Yablonskii, A. S. Mikhailov, K. Nakano, M. Ozaki, and K. Yoshino, Zh. Eksp. Teor. Fiz. **120**, 109 (2001).

14. L. A. Beresnev and L. M. Blinov, Ferroelectrics **33**, 129 (1981).

15. S. V. Yablonskii, N. Oue, H. Nambu, A. S. Mikhailov, M. Ozaki, and K. Yoshino, Appl. Phys. Lett. **75**, 64 (1999).

16. S. Uto, M. Ozaki, and K. Yoshino, Appl. Phys. Lett. **74**, 117 (1999).

17. I. Kraus, Ch. Bahr, I. V. Chikina, and P. Pieranski, Phys. Rev. E **58**, 610 (1998).

18. P. Pieranski, L. Beliard, J.-Ph. Tournellec, X. Leoncini, C. Furtlehner, H. Dumoulin, E. Riou, B. Jouvin, J.-P. Fenerol, Ph. Palaric, J. Heuving, B. Cartier, and I. Kraus, Physica A **194**, 364 (1993).

19. H. F. Gleeson, L. Baylis, W. K. Robinson, J. T. Mills, J. W. Goodby, A. Seed, M. Hird, P. Styring, C. Rosenblatt, and S. Zhang, Liq. Cryst. **26**, 1415 (1999).

20. Y. Takanishi, K. Hiraoka, V. K. Agrawal, H. Takezoe, A. Fukuda, and M. Matsushita, Jpn. J. Appl. Phys. **30**, 2023 (1991).

21. N. M. Shtykov, J. K. Vij, R. A. Lewis, M. Hird, and J. W. Goodby, Phys. Rev. E **62**, 2279 (2000).

22. J. Hou, J. Schacht, F. Giesselmann, and P. Zugenmaier, Liq. Cryst. **22**, 401 (1997).

23. L. V. Blinov, in *Advances in Liquid Crystals: A Special Volume of Advances in Chemical Physics*, ed. by J. Vij, John Wiley & Sons, New York (2000), Vol. 113, p. 77.

24. S. T. Lagerwall, in *Handbook of Liquid Crystals. Low Molecular Weight Liquid Crystals II*, ed. by D. Demus et al. Wiley-VCH, New York (1998), Vol. 2B, p. 515.

25. L. M. Blinov, L. A. Beresnev, and W. Haase, Ferroelectrics **174**, 221 (1995).

26. T. Carlson, F. M. Leslie, N. A. Clark, Phys. Rev. E **51**, 4509 (1995).